

# To Bucket or not to Bucket? Analyzing the performance and interpretability of hybrid hydrological models with dynamic parameterization

Eduardo Acuña Espinoza <sup>1</sup>, Ralf Loritz <sup>1</sup>, Manuel Álvarez Chaves <sup>2</sup>, Nicole Bäuerle <sup>3</sup>, and Uwe Ehret <sup>1</sup>

<sup>1</sup>Institute of Water and Environment, Karlsruhe Institute of Technology (KIT), Karlsruhe, Germany

<sup>2</sup>Stuttgart Center for Simulation Science, Statistical Model-Data Integration, University of Stuttgart, Stuttgart, Germany

<sup>3</sup>Institute of Stochastics, Karlsruhe Institute of Technology (KIT), Karlsruhe, Germany

**Correspondence:** Eduardo Acuña Espinoza (eduardo.espinoza@kit.edu)

**Abstract.** Hydrological hybrid models have been proposed as an option to combine the enhanced performance of deep learning methods with the interpretability of process-based models. Among the various hybrid methods available, the dynamic parameterization of conceptual models using LSTM networks has shown high potential. We explored this method further to evaluate specifically if the flexibility given by the dynamic parameterization overwrites the physical interpretability of the process-based

5 part. We conducted our study using a subset of CAMELS-GB dataset. First, we show that the hybrid model can reach state-of-the-art performance, comparable with LSTM, and surpassing the performance of conceptual models in the same area. We then modified the conceptual model structure to assess if the dynamic parameterization can compensate for structural deficiencies of the model. Our results demonstrated that the deep learning method can effectively compensate for these deficiencies. A model selection technique based purely on the performance to predict streamflow, for this type of hybrid model, is hence not  
10 advisable. In a second experiment, we demonstrate that if a well-tested model architecture is combined with an LSTM, the deep learning model can learn to operate the process-based model in a consistent manner and untrained variables can be recovered. In conclusion, for our case of study, we show that hybrid models cannot surpass the performance of data-driven methods, and the remaining advantage of such models is the access to untrained variables.

## 1 Introduction

15 Rainfall-runoff models are useful tools to support decision-making processes related to water resources management and flood protection. Over the past decades, hydrological conceptual models have emerged as important tools for these purposes, finding widespread usage in academia, industry and national weather services (Boughton and Droop, 2003). These models, known for their simplicity, computational efficiency, and ability to generalize, encode our understanding of hydrological processes within a fixed model structure. By connecting the various macroscopic storages (also known as buckets) through a network of fluxes,  
20 conceptual models try to emulate the internal processes occurring within a catchment. The accurate representation of these processes relies on calibrated parameters, which are adjusted to achieve consistency with observed data. Examples of widely used conceptual models include Hydrologiska Byrans Vattenavdelning (HBV) (Bergström, 1976), Sacramento (Burnash et al.,

1995), GR4J(Perrin et al., 2003), Precipitation-Runoff Modelling System (PRMS) (Leavesley et al., 1983) and TOPMODEL (Beven and Kirkby, 1979), to name a few. Additionally, there are software tools available, such as Raven (Craig et al., 2020) and 25 Superflex (Dal Molin et al., 2021), which facilitate the creation of customized models tailored to specific basin characteristics and key hydrological processes.

Despite the widespread use of conceptual models, data-driven techniques, particularly long short-term memory (LSTM) (Hochreiter and Schmidhuber, 1997) networks, have recently shown the potential to outperform conceptual models, particularly in large sample model comparison studies (Kratzert et al., 2019b; Lees et al., 2021; Feng et al., 2020). The improvement in 30 performance can be attributed, partly, to the inherent flexibility of LSTM networks, which surpasses the constraints imposed by fixed model structures by effectively mapping connections and patterns through optimization techniques. However, the characteristic that allows LSTMs to excel in performance has also sparked criticism regarding their interpretability (Reichstein et al., 2019), owing to the fact that states, weights and biasses in LSTMs lack clear semantic meaning, making it challenging to discern the underlying reasons for their decision and predictions. In recent years, notable advancements in linking hydrological 35 concepts to the internal states of LSTMs have been made (Kratzert et al., 2019a; Lees et al., 2022), and we seek to further contribute in this research direction.

Reichstein et al. (2019) and Shen et al. (2023) indicate that combining process-based environmental models with ML approaches, into so-called hybrid models, can harness the strengths of both methodologies, leveraging the improved performance of data-driven techniques while retaining the interpretability and consistency offered by physical models. Among the various 40 approaches proposed by the authors, one method involves the parameterization of physical models using data-driven techniques. Kraft et al. (2022) applied this method, with the idea that replacing poorly understood or challenging-to-parameterize processes with machine learning (ML) models can effectively reduce model biases and enhance local adaptivity. Moreover, their study demonstrated that the hybrid approach achieved comparable performance to process-based models. Feng et al. (2022) followed a similar procedure, in which the parameters of an HBV model were dynamically estimated using a LSTM 45 network. Their study convincingly demonstrates the effectiveness of this approach, revealing its ability to achieve state-of-the-art performance that directly rivals purely data-driven methods when applied to the Catchment Attributes and Meteorology for Large-sample Studies (CAMELS) data set (Addor et al., 2017) in the United States (CAMELS-US). In their study, Feng et al. (2022) implemented both static and dynamic parameterization techniques and observed that the latter led to slightly improved performance.

50 The dynamic parameterization of a process-based model is not a new idea. Lan et al. (2020) indicate that, historically, the most common approach to accomplish this is the calibration for different sub-periods. He supports this statement by referencing over 20 studies on this subject published in the last 15 years. According to the authors, this method divides the data into sub-periods, considering seasonal characteristics or clustering approaches, and proposing a set of parameters for each sub-period. The idea is to capture the temporal variations of the catchment characteristics.

55 Using an LSTM to give a dynamic parameterization of a process-based model may be seen as a generalization of this process. Specifically, one uses a recurrent neural network that analyzes a given sequence length, so the proposed parameters are context informed, and reflect the current state of the system. The main difference is that the data-driven parameterization

is much more flexible, as a custom parameterization can be proposed for each prediction, and it is not constrained to a typical small set of predefined sub-periods. Also, one can include as input to the LSTM any information that is considered useful to 60 make an informed parameter inference, even if this is not used later in the conceptual part of the model.

However, it is important to note that Feng et al. (2022) warn about the flexibility of LSTM networks when used for dynamic parameterizations. They posed the hypothesis that, while applying dynamic parameterization increases the likelihood of achieving high performance, there is a risk of compromising the physical significance of the model, potentially resulting in the system behaving more like an LSTM variant rather than a hydrologically-meaningful model. In other words, model deficits 65 and ill-defined process descriptions might be compensated by the LSTM. Moreover, Frame et al. (2022) argue that adding any type of constraint, physically based or otherwise, to a data-driven model is only beneficial when such constraints contribute to the optimization process.

Motivated by the outcomes achieved in the aforementioned articles, our study aims to dig deeper into the coupling of LSTM and conceptual models. We believe that dynamic parameters provided by an LSTM allow the conceptual model to not only 70 adapt to changes in the hydrological regime, which is physically reasonable (Loritz et al., 2018) but also to compensate for inherent deficiencies or oversimplifications within the model structure. More specifically, and guided by the warning given by Feng et al. (2022) and Frame et al. (2022), our study aims to address the following research questions:

- 1. Do conceptual models serve as an effective regularization mechanism for the dynamic parameterization of LSTMs?
- 2. Does the data-driven dynamic parameterization compromise the physical interpretability of the conceptual model?

75 To address the research questions at hand, we have structured our article as follows: In Section 2 we describe the structure and training process of the conceptual, data-driven, and hybrid models employed in this study. Additionally, we outline the details of the dataset used to train and test the rainfall-runoff models. In Section 3, after proving that the hybrid model performance is comparable with the LSTM, we conduct experiments to answer our first research question. By systematically modifying the conceptual model, we assess how different forms of regularization affect the overall performance of the hybrid model. This 80 will allow us to better understand the effect of different conceptual models as regularization and the interaction between the data-driven and conceptual components. Furthermore, to address the second research question, we analyze the internal states of the conceptual model to evaluate how much physical interpretability the different variants of our conceptual model is keeping. Finally, we summarize our key findings in Section 4.

## 2 Data and Methods

85 To answer the research questions stated in the previous section we compared three types of models: purely data-driven, stand-alone process-based models and the hybrid approach. The first two types served as baselines in the different experiments we performed for the latter.

The first subsections of this unit present an overview of the dataset utilized for training and testing our models. The second subsection describes the dataset used to evaluate the internal states of our process-based models. The last three segments  
90 explain the structure and training process of the different models.

## 2.1 CAMELS-GB

To train and test our rainfall-runoff models we used the CAMELS-GB dataset (Coxon et al., 2020). This dataset contains information about river discharge, catchment attributes, and meteorological time series for 671 catchments in Great Britain.

Our purely data-driven method consisted of an LSTM network. To be consistent with existing benchmarks, we trained our  
95 LSTM model following the study of Lees et al. (2021). We used the same set of hyperparameters and basins. The importance of building up new studies on community benchmarks is discussed in detail by Kratzert et al. (2024).

To train both the hybrid and conceptual models, as well as to carry out the different comparisons, we selected a subset of basins. This subset was based on an inherent limitation of conceptual models, which in principle does not affect data-driven techniques. Unlike LSTM networks, which learn directly from the data without a predefined structure, conceptual models have  
100 fixed model architectures designed to represent specific processes. This means that anthropogenic impacts such as reservoir operations, withdrawals, or transfers may not be adequately captured by conceptual models unless they are directly accounted for. While this limitation is a clear advantage of data-driven techniques, we aimed to ensure a fair comparison between the models on a level playing field. Therefore, as a first filter, we selected only basins with the label "benchmark\_catch=TRUE" which, according to Coxon et al. (2020), can be treated as "near-natural". In other words, catchments in which the human  
105 influence in flow regimes is modest and where natural processes predominantly drive the flow regimes.

As a second filter, we considered the temporal resolution of the data and the size of the catchment. The CAMELS-GB dataset contains data with a daily resolution. Consequently, we need to consider catchments with a sufficient size such that discharge variations are resolved by daily data. After applying the aforementioned filters, we identified 60 basins that passed both criteria. Figure 1a shows the locations of these basins in the UK. For detailed information on the specific basin IDs please refer to the  
110 supplemental information provided with this article. As indicated before, these 60 catchments were used to train the conceptual and hybrid models, and to compare the performance among the three modeling approaches.

To facilitate the comparison of our results with the studies of Lees et al. (2021) and Lees et al. (2022) we maintained the periods for training (01/10/1980 - 31/12/1997), validating (01/10/1975 - 30/09/1980) and testing (01/01/1998 - 31/12/2008) from their studies.

115 Lastly, we would like to highlight that even though our filtering criteria reduced the size of our original dataset, we still used 60 basins and 28 years of data (training + testing) per basin to conduct our study, which we suggest is sufficiently large to draw robust conclusions from our study results. Furthermore, the spatial distribution of the selected catchments covers most of the original range. Moreover, our models' performance, as demonstrated later, aligns with the benchmark set by Lees et al. (2021) for the CAMELS-GB full dataset, further validating the robustness of our methods. Lastly, as mentioned in the introduction  
120 and elaborated in subsequent sections, besides the data-driven and hybrid models, we also trained the conceptual models. Therefore, using a subset of the original dataset played an important role in maintaining a moderate computational cost.

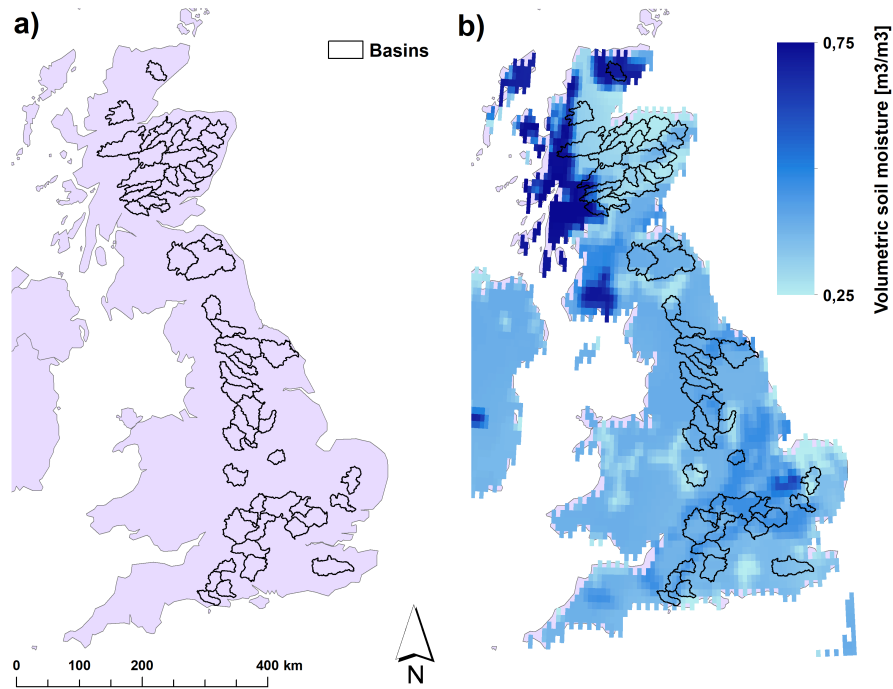


**Figure 1.** a) Location of the 60 basins selected from CAMELS-GB to carry out the experiments b) Example of ERA5-Land Soil Water Volume information

## 2.2 ERA5-Land

As outlined in the introduction, one of the primary objectives of this study is to assess the physical consistency of our hybrid model. To achieve this, we conducted several tests, one of which involved comparing the unsaturated zone reservoir of the conceptual model with soil moisture estimates (details in section 3.3). Following the procedure proposed by Lees et al. (2022)), we compared our model's results with data from ERA5-LAND (Muñoz Sabater et al., 2021). This dataset, based on a 9 km x 9 km gridded format (see Figure 1b), is a land component reanalysis of the ERA5 dataset (Hersbach et al., 2020). According to Lees et al. (2022), reanalysis data offers several advantages, including longer time series availability, easy transferability to basin-average quantities (consistent with the CAMELS-GB process) due to the gridded format, and global coverage, enabling its application in various locations. As our study region and testing period aligns with that of Lees et al. (2022), we utilized the NetCDF file provided by the authors, which was publicly accessible. We then extracted the values corresponding to our 60 basins and normalized the data to a [0-1] range for comparative purposes. This normalization approach is consistent with Ehret et al. (2020), where they followed a similar process to assess the realism of the unsaturated zone soil moisture dynamics of a conceptual hydrological model.

ERA5-Land contains information about soil water volume at four different levels. Level 1 (swvl1) provides information at a depth of 0 cm to 7 cm, level 2 (swvl2) from 7 cm to 28 cm, level 3 (swvl3) from 28 cm to 100 cm, and level 4 (swvl4) from

100 cm to 289 cm. When using this information to evaluate our models, we consistently found higher correlations for all cases when compared against swvl3. Therefore, the results reported in Section 3.3 are associated with that depth.

### 2.3 Conceptual hydrological model

140 In this study, we employ a conceptual model named "Simple Hydrological model" (SHM) (Ehret et al., 2020) that is in its essence a slightly altered HBV model. We will use SHM both as a stand-alone benchmark and as an integral component of the hybrid model. A detailed explanation of the model is available in Ehret et al. (2020). Nonetheless, we offer a concise overview of the model's key features. In a slight variation from Ehret et al. (2020) we included a snow module, and the potential evapotranspiration is read directly from the CAMELS-GB dataset.

145 Figure 2 illustrates the overall structure of the model. The model input consists of three forcing variables: Precipitation (**P**) [ $mm \cdot d^{-1}$ ], Temperature (**T**) [ $^{\circ}C$ ], and Potential Evapotranspiration (**ETp**) [ $mm \cdot d^{-1}$ ]. These three quantities were read directly from the CAMELS-GB dataset (Coxon et al., 2020). To emulate the hydrological processes occurring in the basin, the model uses five storage components, namely: snow module, unsaturated zone, fast flow, interflow, and baseflow. Overall, to regulate the fluxes between components, eight parameters need to be calibrated: *dd*, *f\_thr*, *su\_max*,  $\beta$ , *perc*, *kf*, *ki* and *kb* (see 150 units in Table 2).

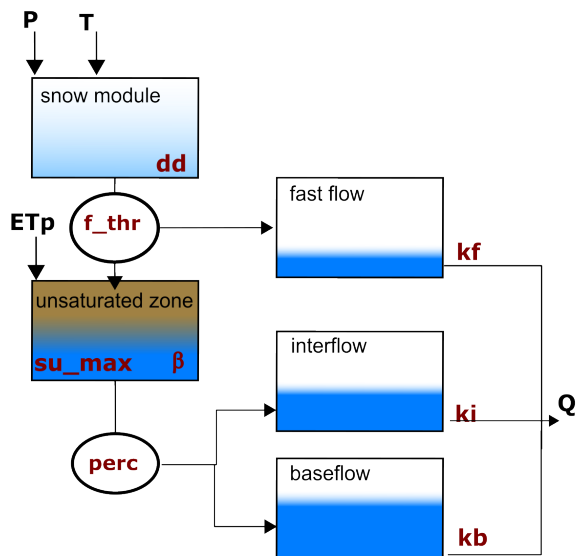


**Figure 2.** Structure of SHM hydrological model used for rainfall-runoff prediction

The snow module receives (**P**) and (**T**) as inputs. Based on the temperature, precipitation is either stored as snow or moves forward together with additional discharge from snowmelt (if any). Snowmelt is calculated using the degree-day method in which the parameter *dd* relates to the volume of snowmelt at a given temperature. If the outflow of the snow module exceeds a

threshold ( $f_{thr}$ ), the excess is directed to the fast flow reservoir while the remaining portion enters the unsaturated zone bucket.

155 On the other hand, if the snow storage outflow is smaller than  $f_{thr}$ , all water enters the unsaturated zone as input. Within the unsaturated zone, several processes occur. First, evapotranspiration causes water loss. The potential evapotranspiration (**ETp**) is provided as a forcing variable but is adjusted to reflect the actual evapotranspiration considering water availability. Additionally, there is an outflow from the unsaturated zone, determined by a power relationship involving the parameters  $su\_max$  and  $\beta$ . This outflow is then divided by the  $perc$  parameter, allocating portions to the inflows of the interflow and baseflow storages. Finally, 160 the total discharge of the basin is computed as the sum of the outflows from the fast flow, interflow, and baseflow storages. Each outflow is a linear function of its corresponding storage and the recession parameters  $kf$ ,  $ki$ , and  $kb$ , respectively.

To establish a benchmark for comparing our data-driven and hybrid methods, we performed individual calibrations of the SHM for each specific basin of interest (e.g. 60 SHM models). This approach is in line with Kratzert et al. (2019b), Nearing et al. (2021) and Kratzert et al. (2024), who indicate that conceptual models generally perform better when calibrated at the 165 individual basin level rather than using a regional calibration approach. To ensure a fair comparison and mitigate potential calibration biases that may favour our hybrid model, we employed three established calibration methods and selected the one that yielded the best performance for each basin. We used Shuffled Complex Evolution (SCE-UA) (Duan et al., 1994), Differential Evolution Adaptive Metropolis (DREAM) (Vrugt, 2016), and Robust Parameter Estimation (ROPE) (Bárdossy and Singh, 2008), all implemented within the Spotpy library (Houska et al., 2015).

## 170 2.4 LSTM

As mentioned in previous sections, we incorporated an LSTM model as a benchmark for our comparison. For a comprehensive understanding of the internal workings of LSTM networks, we refer to the work by Kratzert et al. (2018). In this subsection, we will provide an overview of the key aspects required to comprehend the training process. Our data-driven model was implemented using the PyTorch library (Paszke et al., 2019), and the corresponding code can be found in the repository 175 accompanying this paper.

The model architecture and hyperparameters align with Lees et al. (2021) and Lees et al. (2022). We used a single LSTM layer with 64 hidden states, a dropout rate of 0.4, an initial learning rate of 1e-3 and a sequence length of 365 days. The batch size was set to 256 and the initial bias of the forget gate to 3. Additionally, the ADAM algorithm was used for the optimization.

We also maintained as input three dynamic forcing variables (precipitation, potential evapotranspiration and temperature), 180 along with the same 22 static attributes proposed in the original studies, which encode key characteristics of the catchments. The model output was compared against the observed specific discharge. Following common ML practices, both the input and output data were standardized using the global mean and standard deviation of the training dataset.

To train the LSTM we used the basin-averaged Nash-Sutcliffe Efficiency ( $NSE^*$ ) loss function proposed by Kratzert et al. (2019b). This function divides the squared error between the modelled and observed output by the variance of the specific 185 discharge series associated with each respective basin in the training period. As described by the authors,  $NSE^*$  provides an objective function that reduces bias towards large humid basins during the optimization process, avoiding the underperformance of the regional model in catchments with lower discharges. Given that we are training our regional model for a batch size

$N = 256$ , the training loss was calculated according to equation 1:

$$NSE^* = \frac{1}{N} \cdot \sum_{i=1}^N \frac{(y_i^{obs} - y_i^{sim})^2}{(s_i + \epsilon)^2}, \quad (1)$$

190 where  $y_i^{obs}$  is the observed discharged (standardized),  $y_i^{sim}$  the simulated discharged (standardized),  $s_i$  the standard deviation of the flow series (in training period) for the basin associated with element  $i$ , and  $\epsilon$  is a numerical stabilizer ( $\epsilon = 0.1$ ) so the loss function remains stable even when basins with low flow standard deviations are considered.

## 2.5 Hybrid model: LSTM+SHM

195 Our hybrid model was created by combining an LSTM network, with the same architecture as the one from the previous section, with the SHM. The LSTM network predicts a set of values that serve as parameters for the SHM for each simulation time step. These parameter values are then utilized by the SHM to simulate the discharge, as indicated in Figure 3.

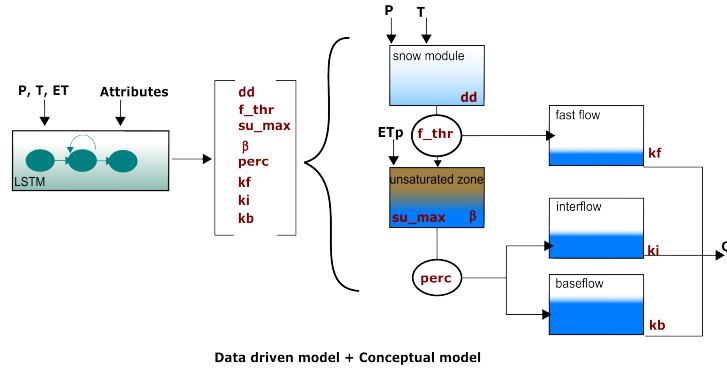


**Figure 3.** Structure of the hybrid hydrological model: LSTM+SHM

An alternative way to interpret the hybrid model is to see the conceptual model as a head layer on the LSTM. As we see in Table 1, in our stand-alone LSTM we require a dense layer (e.g. fully connected linear layer) to translate the information contained in the hidden states into a single output signal. In the LSTM+SHM case, a dense layer is still used to convert the 200 hidden states into as many output signals as parameters in the conceptual model. However, these signals are further processed using the conceptual model to obtain the final discharge. One of the hypotheses that will be tested in the following sections is if the further processing of the signals through the conceptual structure allows us to recover information about non-target variables, e.g. soil moisture.

While the coupling of the data-driven and conceptual models may appear straightforward from a general perspective, it is 205 important to highlight several details. First, as one can notice from Figure 3, the forcing variables (P, T, ET) are used as inputs for both the LSTM and the SHM. The forcing variables and static attributes used as inputs for the LSTM are standardized using the method described in the previous section. However, due to the mass-conservative structure of the SHM, their input variables (P, T, ET) are used in the original scale. Second, it is important to consider that the SHM parameters have certain

**Table 1.** Visualization of hybrid models as head layers of data-driven methods

Model	Neural Network	Head Layer	Output
LSTM	LSTM	Dense	Q
LSTM+SHM	LSTM	Dense+SHM	Q
LSTM+Bucket	LSTM	Dense+Bucket	Q
LSTM+NonSense	LSTM	Dense+NonSense	Q

feasible ranges. While the LSTM could theoretically learn these ranges, the optimization process becomes highly challenging  
210 due to the immense search space involved. We found that without constraining the parameter ranges, the LSTM was not able to identify parameters that yield a functional hydrological model. Hence, we predefined ranges within which the parameters can vary (see Table 2). These ranges were defined considering the findings in Beck et al. (2016) and Beck et al. (2020), which provide valuable insights into the appropriate parameter values of conceptual models. By defining these ranges, we not only reduced the computational costs of the optimization but also ensure consistency with the methodology employed by Feng et al.  
215 (2022).

To map the output of the LSTM network to the predefined ranges, the  $j$  outputs ( $j = 8$ , one per parameter) are passed through a sigmoid layer to transform the values to a  $[0, 1]$  interval. Then the transformed values are mapped to the predefined ranges through a min-max transformation, as exemplified in equation 2:

$$\theta_j = x_j^{\min} + \text{sigmoid}(o_j) \cdot (x_j^{\max} - x_j^{\min}), \quad (2)$$

220 where  $\theta_j$  is each of the values passed as parameters to the SHM,  $o_j$  are the original outputs of the LSTM network, and  $x_j^{\min}$  and  $x_j^{\max}$  correspond to the minimum and maximum values of the predefined ranges (see Table 2) in which each parameter can vary, respectively.

225 Lastly, there is a difference in how we trained our LSTM and hybrid model. The first one was trained using a seq2one approach, while the second one used a seq2seq methodology. Furthermore, even though both models used a spin-up period (e.g. sequence length), the spin-up period of the hybrid model also considered a time to stabilize the internal states of the conceptual model.

To facilitate the understanding of the previous concepts let us create an example. Let's assume that both the LSTM and the hybrid model were trained on 60 basins and 10 years ( $\sim 3652$  days) of data, even though we know from before that this was not the case.

230 For training the LSTM we use a batch size of  $N = 256$  and a seq2one method. Therefore, to construct each batch we randomly select, without replacement, 256 data points from the total pool of  $3652 \cdot 60 = 219\,120$  training points. For each of the 256 points of our batch, we run our LSTM for a given sequence length (e.g. 365 time-steps) and extract the last simulated value. We then calculate our loss function with a metric that quantifies the difference between the observed and simulated

**Table 2.** Search range for SHM parameters during hybrid model optimization

Parameter	Minimum value ( $x_j^{min}$ )	Maximum value ( $x_j^{max}$ )	Unit
$dd$	0.0	10.0	$mm^{\circ}C^{-1}d^{-1}$
$f\_thr$	10.0	60.0	$mm$
$su\_max$	20.0	700.0	$mm$
$\beta$	1.0	6.0	—
$perc$	0.0	1.0	%
$k_f$	1.0	20.0	$d$
$k_i$	1.0	100.0	$d$
$k_b$	10.0	1000.0	$d$

$mm$  : millimeters,  $^{\circ}C$  : degree celsius,  $d$  : days

values of the 256 training points and backpropagate this loss to update the network weights and biases. To complete an epoch,  
235 we iterate through the  $\frac{219120}{256} = 855$  batches.

In the case of the hybrid model, we train it as a seq2seq approach, therefore, to calculate the loss function we do not only use  
the last element of our simulated sequence but a part of that sequence (e.g. 365 time-steps). Therefore, for the same scenario of  
60 basins and 10 years of data, we have  $\frac{60 \cdot 10 \cdot 365}{365} = 600$  training vectors, each with 365 elements that are used to calculate the  
loss. If we use a batch size of  $N = 8$ , each batch will contain 8 randomly selected vectors with 365 sequential training points  
240 each, so the loss function will quantify the difference of  $365 \cdot 8 = 2920$  simulated and observed values. To complete an epoch  
we iterate through  $\frac{600}{8} = 75$  batches.

The other small difference while training the models is the length of the spin-up period. For the LSTM we use a sequence  
length of 365 days, which means that we run a sequence of 365 days and extract the last value of this sequence to calculate  
the loss. The first 364 days help us consider the historical information to make a good prediction, and to avoid bias due to the  
245 initialization of the cell states (usually zero). In our hybrid model, the LSTM uses a sequence length of 180 days, which means  
that only after 180 days we start to retrieve the parameters that go into the conceptual model. The purpose of these 180 days  
is the same as before, consider the historical information to make a context-informed parameter estimation and avoid the bias  
due to the initialization of the cell states. However, we also need a warmup period to avoid a biased due to the initialization  
of the different storages of the conceptual part. Therefore, for each instance of the batch, we ran our conceptual model for a  
250 2-year period. The initial year serves solely as a warm-up period (excluded from the loss function), while the second year's  
data is utilized for actual training. Figure 4 illustrates the data handling while training both models.

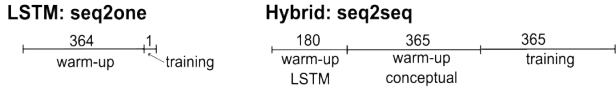


**Figure 4.** Training scheme comparison for LSTM and hybrid model. The former one uses a seq2one approach. The latter uses a seq2seq approach and the total spin-up period consists of a sequence length for the data-driven part plus a warm-up period for the states of the conceptual part.

### 3 Results and Discussion

#### 3.1 Benchmarking our LSTM model

Kratzert et al. (2024) explains the importance of using community benchmarks to test if new ML pipelines are configured appropriately. They suggest that in case the researchers decide to use their own models or different setups, they should first recreate standard benchmarks to make sure that their model is up to date with the current state of the art, and then make the respective changes.

Considering that the stand-alone LSTM model was going to be used as a baseline for all our experiments, we trained our LSTM model architecture on the benchmark established by Lees et al. (2021) for CAMELS-GB and compared its performance against their model. To further validate our architecture, we also trained on the benchmark established by Kratzert et al. (2019b) for CAMELS-US and again compared the performance of our model against theirs. The scope of those two benchmarks is different than the 60 basins used as a testing set for this article and its experiments, but making these comparisons help us validate our ML pipeline.

As we can see in Figure 5, the cumulative distribution functions (CDF) for the Nash–Sutcliffe efficiency (NSE) of the different basins are very much alike. For the case of Great Britain, Lees' model achieved a median NSE of 0.88 while ours reached 0.869. In the case of the US, Kratzert's benchmark reported a median NSE of 0.759 while our model got 0.743. The small differences can be explained by the fact that both benchmark studies make the calculation based on an ensemble of various LSTM models, while we only presented the results for a single run. However, the overall agreement validates our model's pipeline and increases the confidence in the results.

#### 270 3.2 LSTM vs LSTM+SHM

Once we tested our stand-alone LSTM pipeline, the next task was to develop our hybrid model (LSTM+SHM). By following the data and methods outlined in Section 2, we achieved a performance comparable to that of an LSTM. When evaluated across the 60 testing basins, both the LSTM and the LSTM+SHM yielded a median NSE of 0.88. Figure 6 displays the NSE CDF, clearly demonstrating the close performance between both models. In the same figure, we can see that both models outperformed the basin-wide calibration of the SHM model, which achieved a median NSE of 0.76. Additionally, the performance of both models aligns with the reported median NSE of Lees et al. (2021), which indicates that even though we are using a subset of CAMELS-GB for our experiments, the subset is representative of the overall conditions.

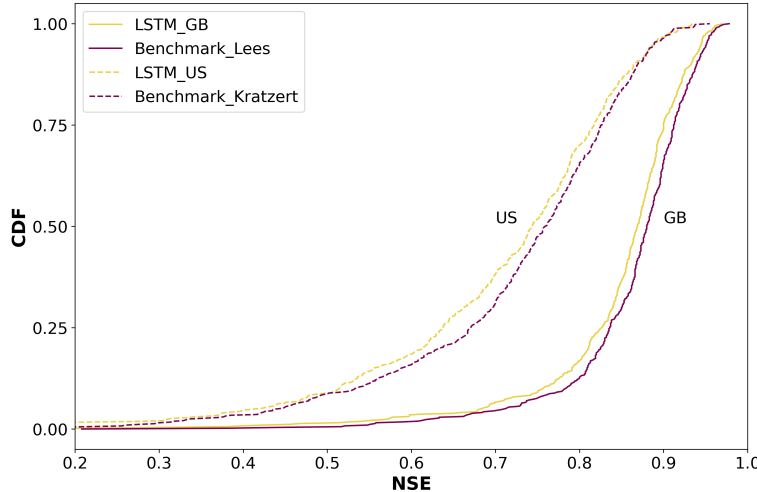


**Figure 5.** Cumulative density functions of the NSE comparing our LSTM model with current state-of-the-art benchmarks

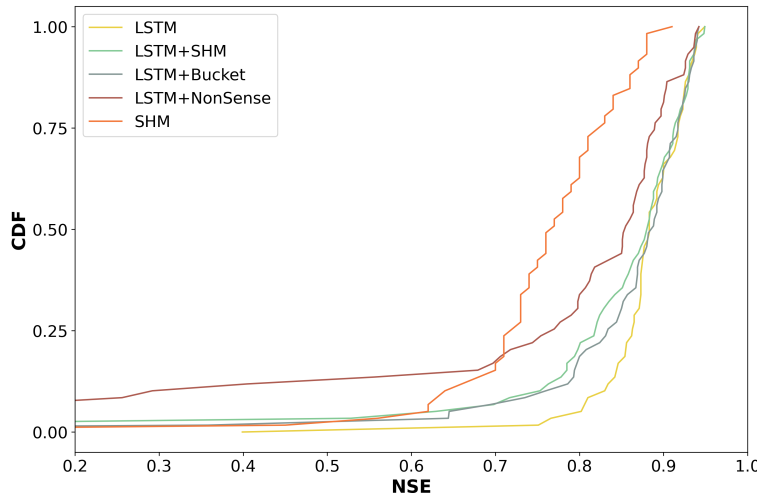


**Figure 6.** Cumulative density functions of the NSE for the different models

One point worth explaining is the decreased performance of our hybrid model compared to the LSTM in the low-performing basins. More specifically, there are four basins (ID 28015, 39010, 42004 and 43008) whose performance in the hybrid model is 280 lower than the rest. Of these four basins, three are also the lowest-performing in the stand-alone SHM model, which suggests a problem with the input data. The LSTM network has the capability to account for biases in the forcing variables (e.g. precipitation or evapotranspiration) because mass conservation is not enforced (Frame et al., 2023). However, both the conceptual and the hybrid approaches have a mass conservative structure, so the input quantities cannot be adjusted. This problem was also reported by Feng et al. (2022) when applied to certain basins in CAMELS-US. It is important to highlight that this issue

285 was observed in only a few basins, and on 90% of the basins the performance of the hybrid approach is fully comparable with the LSTM.

In summary, we observed comparable performance between the LSTM and LSTM+SHM models. Moreover, both models outperformed the SHM-only, which indicates that the dynamic parameterization given by the LSTM is able to improve the predictive capability of the model. This finding aligns with Feng et al. (2022), where they reached a similar conclusion despite  
290 using a different conceptual model and applying it to a different dataset. It also coincides with Hoge et al. (2022) and Kraft et al. (2022), who showed that fusing deep learning methods with hydrological mechanistic models allows reaching state-of-the-art performance. Moreover, it conforms with Mendoza et al. (2015), who argues that fixed parameters can over-constrain a model's ability to make good predictions. However, as described in the introduction, we are interested in looking at the LSTM-SHM interaction, to evaluate if the good performance of the hybrid model is due to the right reasons (Kirchner, 2006) and based on a  
295 consistent interaction between the two model approaches, or if the LSTM network is overwriting the conceptual element. This will be explored in the following section.

### 3.3 Effect of different regularizations

The first step to answer the aforementioned research question was to evaluate if the dynamic parameterization given by the LSTM can overcome the regularization imposed by the conceptual model. For this, we conducted two experiments, in which  
300 the structure of the conceptual model was modified. In the first experiment (see Figure 7a), we substituted the SHM with a single linear reservoir, leading to the removal of most hydrological processes typically represented in a conceptual model through different reservoirs and interconnecting fluxes. A single bucket model only assures mass conservation and a dissipative effect in which the input is lagged based on the recession coefficient in combination with a macroscopic storage. As observed in Figure 7a, the model involves two calibration parameters: the recession parameter  $k$  and a factor for the evapotranspiration  
305 term ( $\alpha$ ). Similar to the previous cases, we defined predefined ranges in which the parameters were allowed to vary, with  $k$  in the range [1 - 500] and  $\alpha$  between [0 - 1.5]. Our initial expectation was that if our head layer: a) restricts the flexibility of the LSTM because the output of the LSTM (after our dense layer) is further passed through a one-process (single bucket) layer, and b) the one-process layer encodes almost no hydrological process understanding, then the performance of the model would drop. However this was not the case. The performance of this hybrid model (LSTM+Bucket) is fully comparable to  
310 that of the LSTM and LSTM+SHM, achieving a median NSE of 0.88 (see Figure 6). For reference, when calibrated without dynamic parameterization, the median NSE of the stand-alone bucket model drops to 0.61. This finding indicates that the LSTM's dynamic parameterization effectively compensates for the missing processes, and the regularization provided by the single bucket is insufficient to impact the model's performance.

Given the insights gained from the LSTM+Bucket experiment, we conducted a second experiment introducing an intentionally implausible structure in the conceptual model, referred to as LSTM+NonSense. As shown in Figure 7b, we removed the fast flow reservoir, creating a single flow path comprising the baseflow, interflow, and unsaturated zone, in that specific order. We also maintained the parameter ranges specified in Table 2, which restrict the baseflow reservoir to have smaller recession  
315 times than the interflow. Then, only after the water has been routed through these two reservoirs it can enter the unsaturated

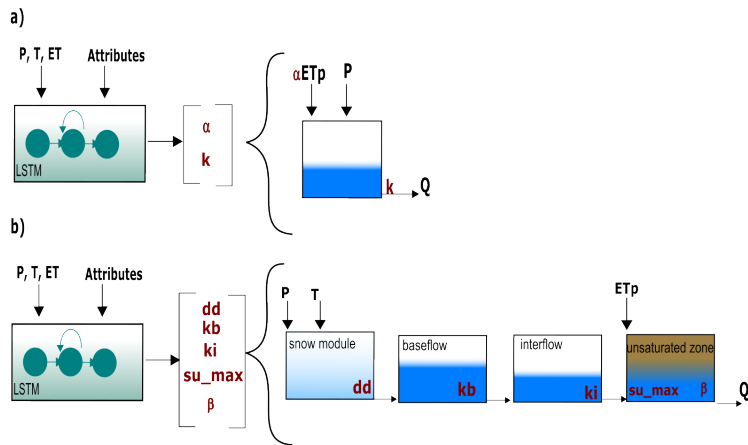


**Figure 7.** Structure of the different regularization: a) LSTM+Bucket b) LSTM+NonSense

zone, where the outflow is no longer controlled by a recession parameter but by an exponential relationship depending on  
 320  $\alpha$  and  $\beta$ . Under static parameterization, the stand-alone NonSense model yielded a median NSE of 0.64, similar to the performance of the stand-alone bucket model. However, after applying dynamic parameterization, the LSTM+NonSense achieved a median NSE of 0.85 (see Figure 6), quite similar to the rest of the hybrid models and surpassing the stand-alone SHM model. During the test we observed that the optimization routines tried to reduce the recession parameter of the baseflow and interflow, to avoid the initial lagging. This caused the optimized parameters to reach the lower limits, which might  
 325 have limited an additional performance increase. Expanding the parameter ranges might lead to a further performance gain, however, this would come at the cost of reducing the differences between the reservoirs, which contradicts the objective of the experiment. Taken together, these experiments provided valuable insights into addressing the first research question posed in the introduction: Can conceptual models effectively serve as a regularization mechanism for the dynamic parameterization given by the LSTMs? Based on our results, we observed that the regularization offered by the conceptual model is not strong  
 330 enough to reduce the hybrid model performance, and the dynamic parameterization given by the LSTM can even compensate for missing processes and implausible structures. Figure 8 highlights that, for some basins, we obtained a similar hydrograph for all models used. Therefore, we recommend being careful about using this hybrid scheme for comparing different types of conceptual models or multiple working hypotheses (Clark et al., 2011), especially if we are evaluating model adequacy by performance alone, as the overall performance can be adjusted by the data-driven part.

335 However, the fact that the data-driven component possesses this capability does not necessarily imply that a well-structured conceptual model cannot be consistently utilized by the LSTM. Our next objective is to further explore this hypothesis, addressing the second research question, as presented in the following section.

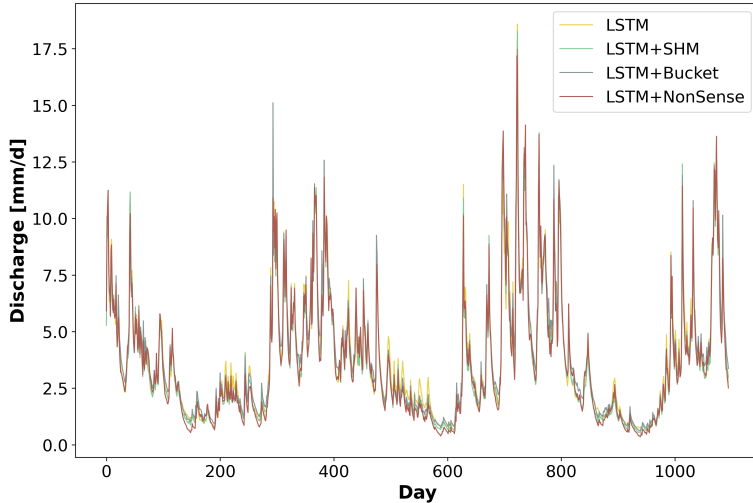


**Figure 8.** Specific discharge series in the testing period for basin ID 15006, simulated by the different models

### 3.4 Analysis of LSTM+SHM

To assess the interpretability of the conceptual part of our LSTM+SHM model, we conducted several tests. Hybrid models, as highlighted by Feng et al. (2022), Kraft et al. (2022) and Hoge et al. (2022), offer the advantage of providing access to untrained variables as the model's states and fluxes have dimensions and semantic meaning. As such, our first test was a model intercomparison. Specifically, we evaluated the filling level of the unsaturated zone reservoir, representing soil moisture in our model (LSTM+SHM), against ERA5-LAND soil water volume information. The process of utilizing reanalysis data and the necessary data processing steps for this comparison are detailed in Section 2.2.

Across the 60 basins in the testing period, the LSTM+SHM model demonstrated a median correlation of 0.86 when compared against the soil moisture simulation provided by ERA5-LAND. This result indicates that the unsaturated zone dynamics are well represented in our model and that the hybrid approach allows us to recover this variable without including any soil moisture information in our training.

Lees et al. (2022) present an alternative method to extract non-target variables from data-driven techniques. They train a model (which they call a probe) to map the information contained in the cell states of the LSTM to a given variable. Specifically, they trained an LSTM using CAMELS-GB, mapped the soil moisture information using a probe and evaluated their outcome against ERA5-LAND data. Because our testing period was aligned with their experiment, we were able to directly compare their results to ours.

When we evaluated Lees' method in our 60 testing basins, his probes got a correlation against ERA5-LAND data of 0.9, surpassing our median correlation of 0.86. Figure 9 shows a more detailed comparison. Both methods got similar results in basins with high correlation, however, Lees' method was more robust in low-performing basins. This effect can be directly linked to the explanation we gave above when a similar behaviour was observed when predicting discharge. The LSTM network

can account for biases in the forcing variables because mass conservation is not enforced, while our hybrid approach is limited by their mass conservative structure.

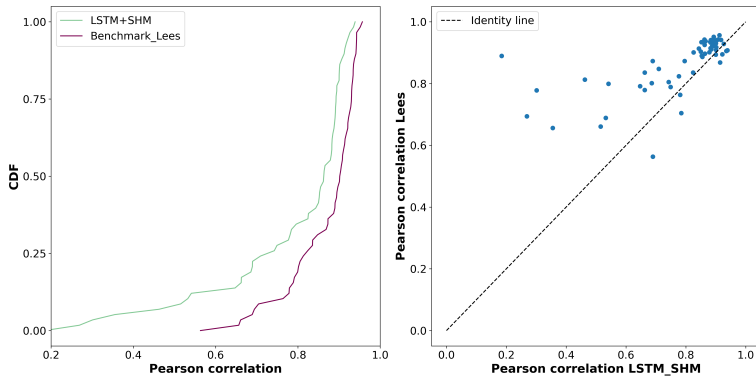


**Figure 9.** Comparison of soil moisture estimates using our hybrid approach method and Lees et al. (2022) approach. The simulated results of both approaches were compared against ERA5-Land data. Left: CDF for the correlation coefficient obtained by both models when applied to the testing dataset. Right: Comparison of correlations provided by both models.

360 The main difference with Lees et al. (2022) is that their probe to extract non-target variables needs to be trained, while in our hybrid approach, no extra training needs to be done. The fact that in Lees et al. (2022) the probe can be as simple as a linear model, which requires few points to train, is not being argued, and in many cases, this will reduce the advantage given by our method.

365 Lastly, it is important to note that the correlation obtained by the LSTM+Bucket (0.85) and LSTM+NonSense (0.82) models is still high, which can be attributed to the strong dependence of soil moisture with the precipitation and evapotranspiration series, both of which serve as boundary conditions for all models. This point also highlights our previously stated concern about using hybrid models for comparing different types of conceptual models or multiple working hypotheses.

370 In addition to the comparison with external data, we also examined the correlation between soil moisture estimates produced by the LSTM+SHM model and the stand-alone SHM. The median correlation value of 0.97 further confirms that the unsaturated zone within our hybrid model operates under our initial expectations. Figure 10 exemplifies this agreement for basin 11001, where the modelled (LSTM+SHM) and ERA5-LAND series exhibit a correlation of 0.86, equivalent to the median correlation observed across all 60 basins. For reference, the median correlation of the stand-alone SHM over the 60 basins was 0.87

375 The last experiment to further evaluate the consistency of our hybrid model was to analyze the parameter variation over time. Figure 11 presents the results for four calibration parameters:  $su_{max}$ ,  $\beta$ ,  $kb$ , and  $ki$ , across two different basins (reasons for choosing these two basins are explained below). We begin by examining the behaviour of the first two parameters.

The purpose of  $su_{max}$  and  $\beta$  is to control the water transfer from the unsaturated zone reservoir to the interflow and baseflow, following equation 3:

$$qu_{out} = qu_{in} \cdot \left( \frac{su}{su_{max}} \right)^\beta, \quad (3)$$

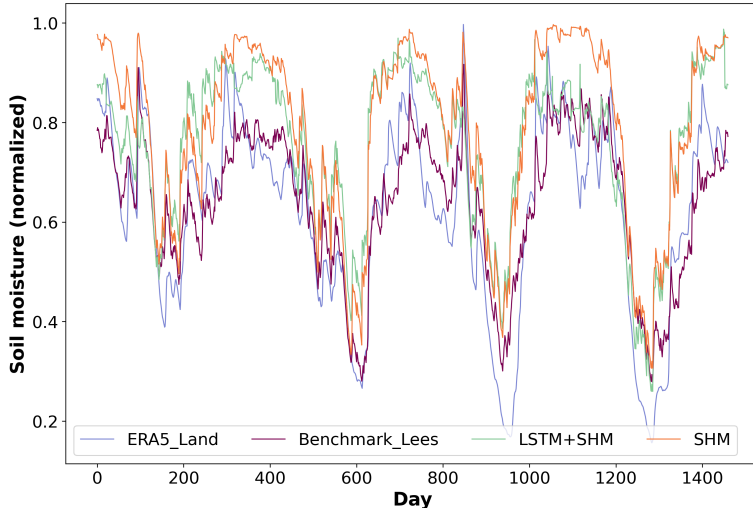


**Figure 10.** Soil moisture time series comparison during the testing period for basin ID 11001

where  $qu_{-out}$  represents the water going out of the unsaturated zone,  $qu_{-in}$  represents the water entering the unsaturated zone from precipitation and snowmelt,  $su$  refers to the unsaturated zone storage or soil moisture, and  $su_{-max}$  and  $\beta$  are the calibration parameters. It is important to note that the value of  $su$  cannot exceed  $su_{-max}$ , which forces their quotient to be less or equal to one. Consequently, a larger value of  $su_{-max}$  and/or  $\beta$ , leads to a decrease in the unsaturated zone outflow.

The parameter variation in basin id 15016 presents clear seasonal patterns. During low-flow periods, both parameters increase, resulting in reduced water availability for the remaining two reservoirs, and, consequently, a decrease in the total outflow. On the other hand, during high-flow periods, the opposite happens. As both parameters decrease, there is an increase in water availability, resulting in higher outflows.

Regarding the other two parameters,  $kb$ , and  $ki$  have a linear relationship with their respective outflows, acting as the denominator of their storage units ( $q_{[i,b]} = \frac{su_{[i,b]}}{kb_{[i,b]}}$ ). For  $kb$ , we can observe seasonal patterns, which allows the model to further increase the baseflow in wet periods and reduce it during dry seasons. This also aligns with our knowledge that hydraulic conductivity is lower when the soil is drier. On the contrary,  $ki$  displays faster variations.

Basin 9002 shows high-frequency variability for most of the parameters, but still a good agreement between the observed and simulated discharge. This basin also exhibits a big increase in performance when the dynamic parameterization is applied, achieving an NSE of 0.91 for the LSTM+SHM against an NSE of 0.73 for the stand-alone SHM. This boost in performance when the dynamic parameterization is applied, is almost 4 times as high as the equivalent scenario for basin 15016. We argue this is the base for explaining the high-frequency variability we see in the figure.

In a hypothetical case in which we have a ‘perfect’ conceptual model, that considers all the processes happening in the basin, the predicted parameters will be constant. However, due to structural limitations of the conceptual architecture, the LSTM does take part in the predicting. Because of how the LSTM and the conceptual model are connected, the only way for the former

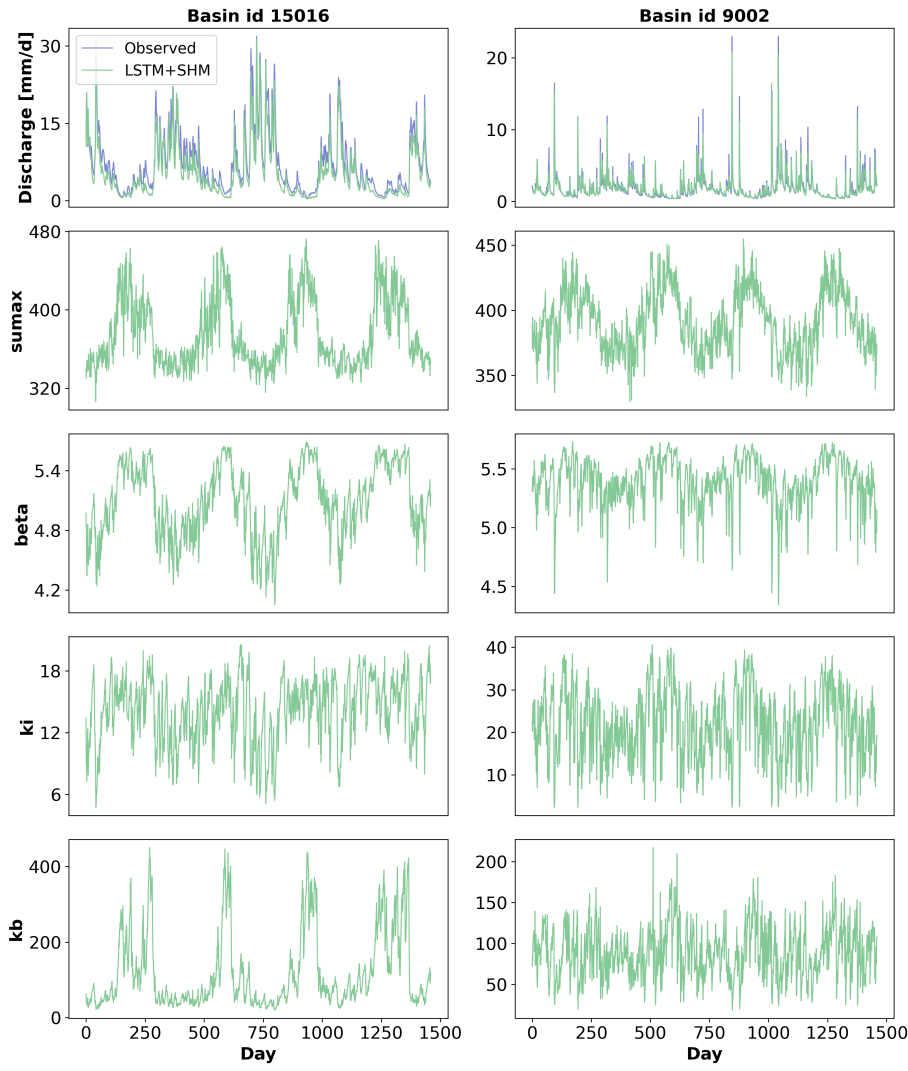


**Figure 11.** Time variation of parameters for basins 15016 (left column) and 9002 (right column). It should be noted that the Y-Axis ranges of the two basins differ.

to pass ‘predicting information’ to the latter is through the parameters. Some deficiencies can be compensated with a more  
 400 seasonal pattern while others need faster pulses.

An alternative approach is to increase the complexity of our process-based part, reducing the necessity of the data-driven method to compensate for structural deficiencies. For example, Feng et al. (2022) represent the catchment processes using 16 HBVs acting in parallel, which are parameterised through an LSTM. In their case, the recession parameters were predicted as constant in time, and the necessary flexibility to get state-of-the-art performance and account for missing sub-processes was  
 405 considered by the semi-distributed format.

It is worth considering that the bigger and more complex a process-based model is, the more similar it can become to an LSTM. More buckets generate higher flexibility, which can account for more complex process representation, such as different processes, multiple residence times and mass transfers. Moreover, these buckets are normally updated considering some input and output fluxes and some losses. In an LSTM each cell state can be interpreted as a bucket, which can be modified by a 410 forget gate, input gate and (indirectly) output gate. The main difference is that the gates in the LSTM depend on the input and the previous hidden states, and in conceptual models, for simplicity, we usually take these as constants. However, this can be modified by making the gates of the buckets context-dependent, and then both models would be alike. Therefore, regularizing a hybrid model with a complex conceptual model will probably reduce the work that needs to be done by the LSTM, but the final product will not be that different from having just a stand-alone LSTM.

#### 415 4 Summary and Conclusions

In recent years, the idea of creating hybrid models by combining data-driven techniques and conceptual models has gained popularity, aiming to combine the improved performance of the former with the interpretability of the latter. Following this line of thought, Feng et al. (2022) used as a hybrid approach the parameterization of a process-based hydrological model by an 420 LSTM network. The authors demonstrated the potential of the technique to achieve comparable performance as purely data-driven techniques and outperform stand-alone conceptual models. Kraft et al. (2022) also achieved promising results following a similar process.

Motivated by this outcome, our article dug into the effect of dynamic parameterization in our conceptual model, and the consequences this might have on the interpretability of the model. More specifically, we tried to answer the questions: 1. Do conceptual models effectively serve as a regularization mechanism for the dynamic parameterization given by the LSTMs? 425 2. Does the dynamic parameterization of the data-driven component overwrite the physical interpretability of the conceptual model?

The first step towards answering these questions was to create a hybrid model. We coupled an LSTM network with a conceptual hydrological model (SHM), using the former as a dynamic parameterization of the latter. In our study, we demonstrated that our hybrid approach (LSTM+SHM) was able to achieve state-of-the-art performance, comparable to purely data-driven 430 techniques (LSTM). Both models were trained in a regional context, using the CAMELS-GB dataset. The median NSE obtained by both models was 0.88, outperforming the basin-wise calibrated conceptual model, which served as the baseline and achieved a median NSE of 0.76. These findings align with existing literature. For instance, Feng et al. (2022) reached similar conclusions when applying a hybrid model to the CAMELS-US dataset.

Having accomplished a well-performing hybrid model, we addressed the first research question. By modifying the regularization given by the conceptual model, we tested to which degree the dynamic parameterization given by the LSTM has the potential to compensate for missing processes. We proved that a hybrid model composed of an LSTM plus a single bucket (LSTM+Bucket) was able to achieve the same performance as the LSTM+SHM and LSTM-only. This indicates that the regularization given by the conceptual model is not strong enough to drop the predictive capability of the hybrid model, and missing

processes are outsourced to the data-driven part. We also demonstrated that if we use an intentionally implausible structure

440 (LSTM+NonSense), the LSTM also has the flexibility to artificially increase performance.

However, the fact that the data-driven component possesses this capability does not necessarily imply that a well-structured conceptual model cannot be consistently utilized by the LSTM. Therefore, we further analyzed the internal functioning of our LSTM+SHM model, to answer our second research question. We compared the soil moisture predicted by our hybrid model with data from ERA5-LAND. This test addressed one of the main benefits of hybrid models over purely data-driven ones, which 445 is their ability to predict untrained states. Across our testing set, comprised of 60 basins, we obtained a median correlation of 0.86 between our simulated soil moisture and the ERA5-LAND data. This result indicates that our hybrid model was able to produce coherent temporal patterns of the untrained state-variables, without having access to the corresponding data during the training period. We also compared the unsaturated zone reservoir of the LSTM+SHM against the unsaturated zone of the stand-alone SHM, which reported a median correlation of 0.97. These results indicate that the dynamic parameterization was 450 operating the unsaturated zone reservoir in a consistent manner and according to our initial expectations. The last section of the study presented the results of the dynamic parameterization for two basins, where we showed that the high-frequency variations of the parameter's time series are caused by the LSTM trying to compensate for structural deficiencies in our process-based model.

We summarize the key findings of our study as follows:

455 – 1. Do conceptual models serve as an effective regularization mechanism for the dynamic parameterization of LSTMs?

No. Our initial expectation was that if our head layer a) restricts the flexibility of the LSTM and b) the process layer encodes almost no hydrological understanding, then the performance of the model would drop, however, this was not the case. This indicates structural deficiencies in the architectures can be compensated by the data-driven part. Therefore, 460 we recommend being careful about using this hybrid scheme for comparing different types of process-based models, especially if we are evaluating model adequacy by performance alone, as the overall performance can be adjusted by the data-driven part.

– 2. Does the data-driven dynamic parameterization compromise the physical interpretability of the conceptual model?

Partially. We showed that a well-structured conceptual model maintains certain interpretability and even gives us access to untrained variables. However, we also showed that even with a well-structured conceptual model, the LSTM is going 465 to compensate for missing processes and structural limitations, especially when the architecture of the process is not well suited for a specific case. Increasing the complexity of the process-based model would result in less intervention of the data-driven part, however, we argue that the more complex a process-based model is, the more similar it will be to an LSTM network.

– To Bucket or not to Bucket?

470 In our experiments we were not able to increase the performance of the data-driven models by adding a conceptual head layer, and even though the mean performance of the different models was the same, purely data-driven methods showed

better results in low-performing basins. Therefore, until this point, the remaining advantage is the access to non-target variables, which other authors have accomplished with the use of probes. In future research, we will conduct other experiments to evaluate the performance of hybrid models under different conditions, but until this point, we do not have evidence that adding buckets gives a considerable advantage over purely data-driven techniques.

475

*Code availability.* The codes used to conduct all the analyses in this paper are publicly available at: <https://github.com/KIT-HYD/Hy2DL/tree/main>

*Data availability.* The CAMELS US dataset is freely available at the homepage of the NCAR. The CAMELS GB dataset is freely available at <https://doi.org/10.5285/8344e4f3-d2ea-44f5-8afa-86d2987543a9>. All the data generated for this publication can be found at <https://github.com/KIT-HYD/Hy2DL/tree/main>

480

*Author contributions.* The original idea of the manuscript was developed by all authors. The codes were written by E.A.E with support from R.L and M.A.Ch. The simulations were conducted by E.A.E. Results were further discussed by all authors. The draft of the manuscript was prepared by E.A.E. Reviewing and editing was provided by all authors. Funding was acquired by U.E and N.B. All authors have read and agreed to the current version of the manuscript.

*Competing interests.* Some authors are members of the editorial board of HESS.

485

*Acknowledgements.* We would like to thank Dr. Marvin Höge and M.Sc María Fernanda Morales Oreamuno for their valuable input. We would also like to thank the referees, one who remained anonymous and Grey Nearing, as their input in the review process allowed us to produce a better manuscript. Lastly, we would like to thank the Google Cloud Program (GCP) Team, for awarding us credits to support our research and run the models.

490

*Financial support.* This project has received funding from the KIT Center for Mathematics in Sciences, Engineering and Economics under the seed funding program. The article processing charges for this open-access publication were covered by the Karlsruhe Institute of Technology (KIT).

## References

Addor, N., Newman, A. J., Mizukami, N., and Clark, M. P.: The CAMELS data set: catchment attributes and meteorology for large-sample studies, *Hydrology and Earth System Sciences*, 21, 5293–5313, <https://doi.org/10.5194/hess-21-5293-2017>, 2017.

495 Bárdossy, A. and Singh, S. K.: Robust estimation of hydrological model parameters, *Hydrology and Earth System Sciences*, 12, 1273–1283, <https://doi.org/10.5194/hess-12-1273-2008>, 2008.

Beck, H., van Dijk, A., Roo, A., Miralles, D., McVicar, T., Schellekens, J., and Bruijnzeel, L.: Global-scale regionalization of hydrologic model parameters, *Water Resources Research*, 52, <https://doi.org/10.1002/2015WR018247>, 2016.

Beck, H. E., Pan, M., Lin, P., Seibert, J., van Dijk, A. I. J. M., and Wood, E. F.: Global Fully Distributed Parameter Regionalization Based 500 on Observed Streamflow From 4,229 Headwater Catchments, *Journal of Geophysical Research: Atmospheres*, 125, e2019JD031485, <https://doi.org/https://doi.org/10.1029/2019JD031485>, e2019JD031485 10.1029/2019JD031485, 2020.

Bergström, S.: Development and application of a conceptual runoff model for Scandinavian catchments, Tech. rep., Sveriges Meteorologiska Och Hydrologiska Institut, 1976.

Beven, K. J. and Kirkby, M. J.: A physically based, variable contributing area model of basin hydrology / Un modèle 505 à base physique de zone d'appel variable de l'hydrologie du bassin versant, *Hydrological Sciences Bulletin*, 24, 43–69, <https://doi.org/10.1080/02626667909491834>, 1979.

Boughton, W. and Droop, O.: Continuous simulation for design flood estimation—a review, *Environmental Modelling & Software*, 18, 309–318, 2003.

Burnash, R. et al.: The NWS River Forecast System-catchment modeling., *Computer models of watershed hydrology.*, pp. 311–366, 1995.

510 Clark, M. P., Kavetski, D., and Fenicia, F.: Pursuing the method of multiple working hypotheses for hydrological modeling, *Water Resources Research*, 47, 2011.

Coxon, G., Addor, N., Bloomfield, J. P., Freer, J., Fry, M., Hannaford, J., Howden, N. J. K., Lane, R., Lewis, M., Robinson, E. L., Wagener, T., and Woods, R.: CAMELS-GB: hydrometeorological time series and landscape attributes for 671 catchments in Great Britain, *Earth System Science Data*, 12, 2459–2483, <https://doi.org/10.5194/essd-12-2459-2020>, 2020.

515 Craig, J. R., Brown, G., Chlumsky, R., Jenkinson, R. W., Jost, G., Lee, K., Mai, J., Serrer, M., Sgro, N., Shafii, M., Snowdon, A. P., and Tolson, B. A.: Flexible watershed simulation with the Raven hydrological modelling framework, *Environmental Modelling and Software*, 129, 104728, <https://doi.org/https://doi.org/10.1016/j.envsoft.2020.104728>, 2020.

Dal Molin, M., Kavetski, D., and Fenicia, F.: SuperflexPy 1.3.0: an open-source Python framework for building, testing, and improving conceptual hydrological models, *Geoscientific Model Development*, 14, 7047–7072, <https://doi.org/10.5194/gmd-14-7047-2021>, 2021.

520 Duan, Q., Sorooshian, S., and Gupta, V. K.: Optimal use of the SCE-UA global optimization method for calibrating watershed models, *Journal of Hydrology*, 158, 265–284, [https://doi.org/https://doi.org/10.1016/0022-1694\(94\)90057-4](https://doi.org/https://doi.org/10.1016/0022-1694(94)90057-4), 1994.

Ehret, U., van Pruijssen, R., Bortoli, M., Loritz, R., Azmi, E., and Zehe, E.: Adaptive clustering: reducing the computational costs of distributed (hydrological) modelling by exploiting time-variable similarity among model elements, *Hydrology and Earth System Sciences*, 24, 4389–4411, <https://doi.org/10.5194/hess-24-4389-2020>, 2020.

525 Feng, D., Fang, K., and Shen, C.: Enhancing Streamflow Forecast and Extracting Insights Using Long-Short Term Memory Networks With Data Integration at Continental Scales, *Water Resources Research*, 56, e2019WR026793, <https://doi.org/https://doi.org/10.1029/2019WR026793>, e2019WR026793 2019WR026793, 2020.

Feng, D., Liu, J., Lawson, K., and Shen, C.: Differentiable, Learnable, Regionalized Process-Based Models With Multiphysical Outputs can Approach State-Of-The-Art Hydrologic Prediction Accuracy, *Water Resources Research*, 58, e2022WR032404, 530 https://doi.org/https://doi.org/10.1029/2022WR032404, e2022WR032404 2022WR032404, 2022.

Frame, J. M., Kratzert, F., Klotz, D., Gauch, M., Shalev, G., Gilon, O., Qualls, L. M., Gupta, H. V., and Nearing, G. S.: Deep learning rainfall-runoff predictions of extreme events, *Hydrology and Earth System Sciences*, 26, 3377–3392, https://doi.org/10.5194/hess-26-3377-2022, 2022.

Frame, J. M., Kratzert, F., Gupta, H. V., Ullrich, P., and Nearing, G. S.: On strictly enforced mass conservation constraints for modelling the 535 Rainfall-Runoff process, *Hydrological Processes*, 37, e14 847, 2023.

Hersbach, H., Bell, B., Berrisford, P., Hirahara, S., Horányi, A., Muñoz-Sabater, J., Nicolas, J., Peubey, C., Radu, R., Schepers, D., Sim- 540 mons, A., Soci, C., Abdalla, S., Abellán, X., Balsamo, G., Bechtold, P., Biavati, G., Bidlot, J., Bonavita, M., De Chiara, G., Dahlgren, P., Dee, D., Diamantakis, M., Dragani, R., Flemming, J., Forbes, R., Fuentes, M., Geer, A., Haimberger, L., Healy, S., Hogan, R. J., Hólm, E., Janisková, M., Keeley, S., Laloyaux, P., Lopez, P., Lupu, C., Radnoti, G., de Rosnay, P., Rozum, I., Vamborg, F., Vil- laume, S., and Thépaut, J.-N.: The ERA5 global reanalysis, *Quarterly Journal of the Royal Meteorological Society*, 146, 1999–2049, https://doi.org/https://doi.org/10.1002/qj.3803, 2020.

Hochreiter, S. and Schmidhuber, J.: Long Short-Term Memory, *Neural Computation*, 9, 1735–1780, https://doi.org/10.1162/neco.1997.9.8.1735, 1997.

Hoge, M., Scheidegger, A., Baity-Jesi, M., Albert, C., and Fenicia, F.: Improving hydrologic models for predictions and process understanding using neural ODEs, *Hydrology and Earth System Sciences*, 26, 5085–5102, https://doi.org/10.5194/hess-26-5085-2022, 2022.

Houska, T., Kraft, P., Chamorro-Chavez, A., and Breuer, L.: SPOTting model parameters using a ready-made python package, *PloS one*, 10, e0145 180, 2015.

Kirchner, J. W.: Getting the right answers for the right reasons: Linking measurements, analyses, and models to advance the science of hydrology, *Water resources research*, 42, 2006.

Kraft, B., Jung, M., Körner, M., Koirala, S., and Reichstein, M.: Towards hybrid modeling of the global hydrological cycle, *Hydrology and 550 Earth System Sciences*, 26, 1579–1614, https://doi.org/10.5194/hess-26-1579-2022, 2022.

Kratzert, F., Klotz, D., Brenner, C., Schulz, K., and Herrnegger, M.: Rainfall–runoff modelling using Long Short-Term Memory (LSTM) networks, *Hydrology and Earth System Sciences*, 22, 6005–6022, https://doi.org/10.5194/hess-22-6005-2018, 2018.

Kratzert, F., Herrnegger, M., Klotz, D., Hochreiter, S., and Klambauer, G.: NeuralHydrology – Interpreting LSTMs in Hydrology, pp. 347– 555 362, Springer International Publishing, Cham, https://doi.org/10.1007/978-3-030-28954-6\_19, 2019a.

Kratzert, F., Klotz, D., Shalev, G., Klambauer, G., Hochreiter, S., and Nearing, G.: Towards learning universal, regional, and local hydrological behaviors via machine learning applied to large-sample datasets, *Hydrology and Earth System Sciences*, 23, 5089–5110, 2019b.

Kratzert, F., Gauch, M., Klotz, D., and Nearing, G.: HESS Opinions: Never train an LSTM on a single basin, *Hydrology and Earth System Sciences Discussions*, 2024, 1–19, https://doi.org/10.5194/hess-2023-275, 2024.

Lan, T., Lin, K., Xu, C.-Y., Tan, X., and Chen, X.: Dynamics of hydrological-model parameters: mechanisms, problems and solutions, *Hydrology and Earth System Sciences*, 24, 1347–1366, https://doi.org/10.5194/hess-24-1347-2020, 2020.

Leavesley, G., Lichy, R., Troutman, B., and Saindon, L.: Precipitation-runoff modelling system: user's manual, Report 83–4238, Tech. rep., US Geological Survey Water Resources Investigations, https://doi.org/https://pubs.usgs.gov/wri/1983/4238/report.pdf, 1983.

Lees, T., Buechel, M., Anderson, B., Slater, L., Reece, S., Coxon, G., and Dadson, S. J.: Benchmarking data-driven rainfall-runoff models  
565 in Great Britain: a comparison of long short-term memory (LSTM)-based models with four lumped conceptual models, *Hydrology and Earth System Sciences*, 25, 5517–5534, <https://doi.org/10.5194/hess-25-5517-2021>, 2021.

Lees, T., Reece, S., Kratzert, F., Klotz, D., Gauch, M., De Bruijn, J., Kumar Sahu, R., Greve, P., Slater, L., and Dadson, S. J.: Hydrological concept formation inside long short-term memory (LSTM) networks, *Hydrology and Earth System Sciences*, 26, 3079–3101, <https://doi.org/10.5194/hess-26-3079-2022>, 2022.

570 Loritz, R., Gupta, H., Jackisch, C., Westhoff, M., Kleidon, A., Ehret, U., and Zehe, E.: On the dynamic nature of hydrological similarity, *Hydrology and Earth System Sciences*, 22, 3663–3684, <https://doi.org/10.5194/hess-22-3663-2018>, 2018.

Mendoza, P. A., Clark, M. P., Barlage, M., Rajagopalan, B., Samaniego, L., Abramowitz, G., and Gupta, H.: Are we unnecessarily constraining the agility of complex process-based models?, *Water Resources Research*, 51, 716–728, 2015.

Muñoz Sabater, J., Dutra, E., Agustí-Panareda, A., Albergel, C., Arduini, G., Balsamo, G., Boussetta, S., Choulga, M., Harrigan, S., Hersbach, 575 Martens, B., Miralles, D. G., Piles, M., Rodríguez-Fernández, N. J., Zsoter, E., Buontempo, C., and Thépaut, J.-N.: ERA5-Land: a state-of-the-art global reanalysis dataset for land applications, *Earth System Science Data*, 13, 4349–4383, <https://doi.org/10.5194/essd-13-4349-2021>, 2021.

Nearing, G. S., Kratzert, F., Sampson, A. K., Pelissier, C. S., Klotz, D., Frame, J. M., Prieto, C., and Gupta, H. V.: What role does hydrological science play in the age of machine learning?, *Water Resources Research*, 57, e2020WR028091, 2021.

580 Paszke, A., Gross, S., Massa, F., Lerer, A., Bradbury, J., Chanan, G., Killeen, T., Lin, Z., Gimelshein, N., Antiga, L., et al.: Pytorch: An imperative style, high-performance deep learning library, *Advances in neural information processing systems*, 32, 2019.

Perrin, C., Michel, C., and Andréassian, V.: Improvement of a parsimonious model for streamflow simulation, *Journal of Hydrology*, 279, 275–289, [https://doi.org/https://doi.org/10.1016/S0022-1694\(03\)00225-7](https://doi.org/https://doi.org/10.1016/S0022-1694(03)00225-7), 2003.

Reichstein, M., Camps-Valls, G., Stevens, B., Jung, M., Denzler, J., and Carvalhais, N.: Deep learning and process understanding for data- 585 driven Earth system science, *Nature*, 566, 195–204, 2019.

Shen, C., Appling, A. P., Gentine, P., Bandai, T., Gupta, H., Tartakovsky, A., Baity-Jesi, M., Fenicia, F., Kifer, D., Li, L., et al.: Differentiable modelling to unify machine learning and physical models for geosciences, *Nature Reviews Earth & Environment*, pp. 1–16, 2023.

Vrugt, J. A.: Markov chain Monte Carlo simulation using the DREAM software package: Theory, concepts, and MATLAB implementation, *Environmental Modelling and Software*, 75, 273–316, <https://doi.org/https://doi.org/10.1016/j.envsoft.2015.08.013>, 2016.